Exploring the Properties of Dark Energy Using Type Ia Supernovae and Other Datasets

Ujjaini Alam[a], Varun Sahni[b] and Alexei A. Starobinsky[c]
[a] *International Centre for Theoretical Physics, Strada Costiera 11, 34100 Trieste, Italy*
[b] *Inter-University Centre for Astronomy and Astrophysics, Pune 411 007, India and*
[c] *Landau Institute for Theoretical Physics, 119334 Moscow, Russia*

We reconstruct dark energy properties from two complementary supernova datasets – the newly released Gold+HST sample and SNLS. The results obtained are consistent with standard ΛCDM model within 2σ error bars although the Gold+HST data favour evolving dark energy slightly more than SNLS. Using complementary data from baryon acoustic oscillations and the cosmic microwave background to constrain dark energy, we find that our results in this case are strongly dependent on the present value of the matter density $\Omega_{0\mathrm{m}}$. Consequently, no firm conclusions regarding constancy or variability of dark energy density can be drawn from these data alone unless the value of $\Omega_{0\mathrm{m}}$ is known to an accuracy of a few percent. However, possible variability is significantly restricted if this data is used in conjunction with supernova data.

INTRODUCTION

There is a growing consensus in cosmology that the Universe is currently accelerating. Perhaps the simplest explanation of this property is the presence of a positive cosmological constant Λ. Although Λ appears to explain all current observations satisfactorily, to do so its value must necessarily be very small $\Lambda/8\pi G \simeq 10^{-47}\mathrm{GeV}^4$. So, it represents a new small constant of nature in addition to those known from elementary particle physics. However, since it is not known at present how to derive it from these other small constants and it is even unclear if it should be exactly constant, other phenomenological explanations for cosmic acceleration have been suggested. Collectively called *dark energy* (DE) models, they are based either on the introduction of new physical fields (quintessence and phantom models, the Chaplygin gas, etc.), or on *geometrical approaches* which attempt to generate acceleration by means of a change in the laws of gravity and, therefore, the geometry of space-time [1]. Scalar-tensor gravity, $R+f(R)$ gravity and higher dimensional 'Braneworld' models are prominent members of this second category.

The growing number of DE models has inspired a complementary approach whose aim is to reconstruct properties of DE directly from observations in a quasi-model independent manner, see the recent review [2] and the extensive list of references therein. The aim of this paper is to investigate what new insights can be obtained about DE using the most recent data, and to see whether or not these data strengthen previously obtained results on the closeness of DE to Λ. We study two different supernova samples – the newly released Gold+HST sample [3] and SNLS data [4] – to see what constraints follow from them on possible evolution of DE. We also investigate the possibility of extracting information about the nature of DE from datasets other than the supernova data. To this end, we consider what follows from the value of the R parameter characterizing acoustic peaks in the angular power spectrum of the cosmic microwave background (CMB) [5, 6] and from the SDSS result on the baryon acoustic oscillation peak (BAO) [7].

DATA AND METHODOLOGY

In this paper, we shall compare the reconstruction results for different recent sets of observations. We briefly summarize each of the data sets which we shall use before proceeding to give the results of our comparison.

Type Ia supernova data is the strongest evidence for DE in current cosmology. The data is in the form of $\mu_{0,i}(z_i) = m_B - M = 5\log d_L(z_i) + 25$ with

$$d_L(z) = (1+z)\int_0^z \frac{dz}{H(z)}\ , \tag{1}$$

where $H(z) = H_0 h(z)$ is defined in (8) for the ansatz used.

We use the following two SNe datasets available to us at present.

1. *The Gold+HST data set* : As recently as 2003, the entire supernova dataset from the two different surveys – Supernova Cosmology Project (SCP) and High z Supernova Search Team (HZT), along with low redshift supernovae from Calan-Tololo Supernova Search (CTSS) comprised of a meager 92 supernovae [8, 9, 10], with

very few at high redshifts, $z > 0.7$. The method of data reduction for the different teams was also somewhat different, so that it was not possible to use the supernovae from the two datasets concurrently. The picture changed somewhat dramatically during 2003-2004, when a set of papers from both these teams [11, 12, 13] presented a joint dataset of 194 supernovae which used the same data reduction method. This new data resulted in doubling the dataset at $z > 0.7$. Not all these supernovae could be identified beyond doubt as Type Ia supernovae however, in many cases complete spectral data was not available. In early 2004, Riess *et al.* [14] reanalyzed the data with somewhat more rigorous standards, excluding several supernovae for uncertain classification or inaccurate colour measurements. They also added 14 new high redshift supernovae observed by the Hubble Space Telescope (HST) to this sample. This resulted in a sample known as the 'Gold' dataset. The latest publication from the same team [3] adds a further 10 SNe from HST to the dataset, and excludes data below $cz = 7000km/s$ ($z = 0.0233$) to avoid the influence of a possible local "Hubble Bubble". The final sample now comprises of 135 supernovae (the furthest being at redshift $z = 1.755$) – we call this sample the 'Gold+HST' dataset and use it as our first SNe sample.

2. *The Supernova Legacy Survey SNe data set (SNLS)* : The SuperNova Legacy Survey [15] is an ongoing 5-year project which is expected to yield more than 700 spectroscopically confirmed supernovae below redshift of one. The first two-year results from this survey [4] have provided us with 71 new supernovae below $z = 1$. We shall use these 71 SNe together with the already available low-z supernova data, i.e. a total of 115 SNe, as our second supernova sample.

In [3], the SNLS and Gold datasets have also been merged together for some of the results. Since the standardization techniques of the two teams are somewhat different, as of now, we consider the two samples separately till a better handle on the systematics is obtained.

Although supernova data forms the major observational proof of dark energy, we may try to obtain independent information on the nature of dark energy from the other observational results. Here we look at the following two datasets.

1. Observations of the cosmic microwave background provide us with very accurate measurements, which may be used to gain insight about dark energy [5]. We may use the WMAP 3-year results to get [6]

$$R = \sqrt{\Omega_{0\mathrm{m}}} \int_0^{z_{1\mathrm{s}}} \frac{dz}{h(z)} = 1.70 \pm 0.03 \tag{2}$$

where $h(z) = H(z)/H_0$ is defined in (8) for the ansatz used. For calculating this quantity, we use $\Omega_b h^2 = 0.024$ and $\Omega_{0\mathrm{m}} h^2 = 0.14 \pm 0.02$. To calculate z_{ls} we use a fitting function given in [16]:

$$z_{ls} = 1048[1 + 0.00124(\Omega_b h^2)^{-0.738}][1 + g_1(\Omega_{0\mathrm{m}} h^2)^{g_2}] \ , \tag{3}$$

where the quantities g_1, g_2 are defined as

$$g_1 = 0.078(\Omega_b h^2)^{-0.238}[1 + 39.5(\Omega_b h^2)^{0.763}]^{-1}, \tag{4}$$

$$g_2 = 0.56[1 + 21.1(\Omega_b h^2)^{1.81}]^{-1} \ . \tag{5}$$

2. *The Baryon Acoustic Oscillation Peak* : A remarkable confirmation of the standard big bang cosmology has been the recent detection of a peak in the correlation function of luminous red galaxies in the Sloan Digital Sky Survey [7]. This peak, which is predicted to arise precisely at the measured scale of 100 h^{-1} Mpc due to acoustic oscillations in the primordial baryon-photon plasma prior to recombination, can provide a 'standard ruler' with which to test dark energy models. Specifically, we shall use the value [7]

$$A = \frac{\sqrt{\Omega_{0\mathrm{m}}}}{h(z_1)^{1/3}} \left[\frac{1}{z_1} \int_0^{z_1} \frac{dz}{h(z)} \right]^{2/3} = 0.469 \left(\frac{n}{0.98}\right)^{-0.35} \pm 0.017 \ , \tag{6}$$

where $h(z) = H(z)/H_0$ is defined in (8) for the ansatz used, and $z_1 = 0.35$ is the redshift at which the acoustic scale has been measured. The 3-year WMAP results yield $n = 0.95$ for the spectral index of density perturbations.

We note here that the quantity A measured from the baryon acoustic oscillations appears to be independent of the value of h. However, the quantity R obtained from CMB measurements depends on $\Omega_{0\mathrm{m}} h^2$, and therefore on the

Hubble parameter. Therefore, when using this quantity, we require to either assign some value to h or to marginalize over $\Omega_{0\mathrm{m}}h^2$.

We use χ^2 minimization on the different datasets with

$$\chi^2(H_0, p_j) = \sum_i \frac{[y_{\mathrm{fit},i}(z_i; H_0, \Omega_{0\mathrm{m}}, p_j) - y_i]^2}{\sigma_i^2} \ . \tag{7}$$

Here, y_i is the data at redshift of z_i and σ_i is the uncertainty in the individual y_i, and p_j are the parameters $\Omega_{0\mathrm{m}}, A_1, A_2$ for the ansatz [17]

$$h^2(z) = \frac{H^2(z)}{H_0^2} = \Omega_{0\mathrm{m}}x^3 + A_0 + A_1 x + A_2 x^2 \ , \quad x = 1 + z \tag{8}$$

with $A_0 = 1 - \Omega_{0\mathrm{m}} - A_1 - A_2$ for a flat universe. Note that this ansatz for the Hubble parameter has been tested and found to give accurate results for a variety of cosmological models [18, 19]. Its main features are: (i) it accounts for a matter dominated regime at high redshift, (ii) it is exact for DE being the mixture of a cosmological constant and non-relativistic domain walls and cosmic strings (in other words, for DE consisting of 3 components with with $w = -1$, $w = -1/3$ and $w = -2/3$), (iii) it can satisfactorily emulate DE with an evolving equation of state including Braneworld models and phantom models admitting regions with $w < -1$ (moreover, the DE effective energy density ρ_{DE} may even become negative in such models).

RESULTS

To test the two SNe datasets, we first reconstruct a ΛCDM model with curvature, using the formula

$$d_L(z) = \frac{c(1+z)}{\sqrt{|\kappa|}} \mathcal{S}\left(\sqrt{|\kappa|}\int_0^z \left[(1+z')^2(1+\Omega_{\mathrm{m}}z') - z'(2+z')\Omega_\Lambda\right]^{-1/2} dz'\right) \ , \tag{9}$$

where

$$\begin{aligned}
&\Omega_{\mathrm{m}} + \Omega_\Lambda > 1 \Rightarrow \mathcal{S}(x) = \sin(x), \ \kappa = 1 - \Omega_{\mathrm{m}} - \Omega_\Lambda \\
&\Omega_{\mathrm{m}} + \Omega_\Lambda < 1 \Rightarrow \mathcal{S}(x) = \sinh(x), \ \kappa = 1 - \Omega_{\mathrm{m}} - \Omega_\Lambda \\
&\Omega_{\mathrm{m}} + \Omega_\Lambda = 1 \Rightarrow \mathcal{S}(x) = x, \ \kappa = 1 \ .
\end{aligned}$$

In figure 1 we show results for a ΛCDM model for both the Gold+HST and SNLS datasets. We see that for the Gold+HST data, the dataset prefers a closed universe somewhat over the flat model. The SNLS best-fit, on the other hand, is very close to the flat model.

We next study the two datasets in more detail using ansatz (8). In figure 2 we show the results for the Gold+HST SNe dataset. We marginalize over $\Omega_{0\mathrm{m}} = 0.28 \pm 0.03$ which is the currently accepted value for matter density from SDSS [7] and show the 2σ confidence levels in $A_1 - A_2$ in panel (a). The logarithmic variation of $\rho_{\mathrm{DE}} = A_0 + A_1 x + A_2 x^2$ is shown in panel (b). The variation of the equation of state of DE

$$w(x) = \frac{(2x/3)\ d\ \ln H\ /\ dx - 1}{1\ -\ (H_0/H)^2 \Omega_{0m}\ x^3} \tag{10}$$

is shown in panel (c), and the deceleration parameter

$$q \equiv -\ddot{a}/aH^2 = \frac{H'(x)}{H(x)}\ x - 1 \, , \quad x = 1 + z \tag{11}$$

is plotted in panel (d). We find that the best-fit is somewhat away from ΛCDM, and favours an evolving model of DE, although ΛCDM is still within 2σ of the best-fit. From the deceleration parameter we find the value of the acceleration epoch, which is the redshift at which the universe started accelerating. For the Gold data this transition between deceleration and acceleration occurs between $z_a = 0.32 - 0.48$ at 2σ. The earlier Gold dataset of [14] favoured an evolving DE model starting from $w < -1$ at present and evolving to $w \sim 0$ at $z \sim 1$ (as shown in [20] and numerous subsequent papers), the addition of the 10 new HST data points do not appear to change that result. These results

also agree with the analysis shown in figure 12 of [3], as well as results from the non-parametric approach advocated in [21].

Figure 3 shows the results for the same reconstruction for the SNLS dataset. Once again we marginalize over the matter density. The results in this case are much closer to ΛCDM, the DE equation of state shows very mild evolution. The acceleration epoch is in the range $z_a = 0.41 - 1.0$.

We note here that although we have marginalized over a particular matter density, results from the supernova data are only weakly dependent on $\Omega_{0\mathrm{m}}$. Within the reasonable range $\Omega_{0\mathrm{m}} = 0.22 - 0.34$ (the 2σ limits on the current observations for $\Omega_{0\mathrm{m}}$), the results do not change significantly.

The ansatz (8) is useful not only for reconstructing the DE density but also for determining an important related quantity – the w-probe [22]. As its name suggests, the w-probe provides us with important insights about the equation of state. However, unlike $w(z)$ which is determined by differentiating $H(z)$, the w-probe is related to the *difference* in the value of the Hubble parameter and is defined as follows

$$1 + \bar{w} = \frac{1}{\Delta \ln(1+z)} \int [1 + w(z)] d \ln(1+z) = \frac{1}{3} \frac{\Delta \ln(\rho_{\mathrm{DE}}/\rho_{0\mathrm{c}})}{\Delta \ln(1+z)} \ . \tag{12}$$

Here Δ denotes the total change in a variable between integration limits. It is important to note that the w-probe, when studied over different redshift bins, can give us evidence for the variation of the equation of state from the first derivative of the data alone, i.e. from the DE density. (As demonstrated in [22], $\bar{w}$ is much less sensitive to uncertainties in the value of the matter density than $w(z)$.) Table I shows the value of the w-probe in three redshift bins (approximately equal in $\log(1+z)$) for both Gold+HST and SNLS datasets. We see that for the gold dataset $\bar{w}$ is close to -1 in the low redshift bin, but in the two higher redshift bins $\bar{w}$ is closer to zero. Thus the Gold+HST dataset seems to provide support for the evolution of DE. On the other hand, for the SNLS data, for both redshift bins (upto redshift of unity), $\bar{w}$ is close to -1, showing that this dataset favours the cosmological constant more than Gold+HST.

In a way, the SNLS results contradict the results obtained for the Gold dataset. This fact had been noted for an earlier Gold dataset in [23]. However, the difference is not very large, at 2σ the results from both datasets are consistent with each other. We should also keep in mind the fact that the light-curve standardization of the two datasets is done using different methods, MLCS2k2 for Gold+HST and SALT for SNLS. As shown in [4], different standardization techniques may lead to differences of upto 0.16 magnitude in the data. The discrepancy in cosmological results may therefore be attributed partly to the different standardization techniques. There are also possible effects from other sources in the data, such as systematic noise and K-correction. Therefore it seems that using just the two current SNe datasets, a firm conclusion cannot yet be reached about the nature of DE. We may conclude that while the cosmological constant is more or less consistent with both datasets, evolving DE is still not ruled out.

Next we examine our results for the CMB+BAO data. In figure 4 we show results for this dataset for which the observations are at redshifts $z = 0.35$ and $z = 1089$. We present our results in panels (b), (c) and (d) over the redshift range of $z = 0 - 1.7$ in order to be able to compare with our earlier results obtained using supernova data. The results for a matter density marginalization of $\Omega_{0\mathrm{m}} = 0.28 \pm 0.03$ are reasonably consistent with ΛCDM, the confidence levels for $A_1 - A_2$ are somewhat tighter than those seen for the SNe results (Comparing panel (a) of figures 2, 3, 4). However, unlike the SNe data, the results from CMB+BAO seem to depend much more strongly on the chosen value of the matter density. In figure 5 we show the difference in the results for three different marginalizations of the matter density. In the left hand panels, we marginalize over $\Omega_{0\mathrm{m}} = 0.25 \pm 0.03$, and the data then favours evolving DE which crosses the so-called phantom divide at $w_0 = -1$. In the middle panels, we marginalize over $\Omega_{0\mathrm{m}} = 0.28 \pm 0.03$, the result is a mildly evolving DE model consistent with ΛCDM. The panels to the right show results marginalized over a higher value of the matter density $\Omega_{0\mathrm{m}} = 0.31 \pm 0.03$, which suggests a DE model with practically constant $w > -1$. These results are supported by an analysis of w-probe shown in table II which demonstrates that the redshift dependence of the mean equation of state $\bar{w}$ is sensitive to the value of $\Omega_{0\mathrm{m}}$. Thus, unlike the SNe data, even a very slight difference in $\Omega_{0\mathrm{m}}$ can lead to a significant difference in the degree of evolution of DE for the CMB+BAO dataset. Note that the generic trend of Ω_m dependence is similar to that recently found in [27] where all data (the old Gold+HST sample, the SNLS dataset, WMAP, BAO and others) were analyzed using the Chevallier-Polarski-Linder parametrization of the DE equation of state [28, 29].

Finally we combine the SNe and CMB+BAO data. We use the marginalization $\Omega_{0\mathrm{m}} = 0.28 \pm 0.03$ for the entire dataset. The results are shown for Gold+HST data in figure 6. We see that the parameter space is strongly constrained by the three sets of data,the cosmological constant is consistent with the data, so are mildly evolving DE models. The results from SNLS are shown in figure 7. We see that the results from both sets of SNe data are strikingly similar, this is because the results are very strongly constrained by the CMB+BAO data. Whether the CMB+BAO data should be used in conjunction with the SNe data, given the strong matter density dependence of the former, is

however rather questionable at this point.

CONCLUSIONS

In this paper, we have explored the reconstruction of DE using the most recent and complementary datasets available to us at present. First, we reconstructed DE using two supernova datasets– the recently released Gold+HST dataset and the SNLS two-year dataset. We find that the results for the two are slightly inconsistent. The Gold+HST dataset appears to favour an evolving model of DE with $w_0 < -1$ at present and $w \sim 0$ at $z \sim 1$ over ΛCDM for its best-fit, however ΛCDM is still consistent at 2σ. For SNLS data, the results are more consistent with ΛCDM. It should be emphasized here that we are speaking about DE properties averaged over a redshift interval ~ 0.4 or more, see e.g. Tables I, II. Note also that, as follows from these tables and Figs. 2-7, significantly phantom behaviour of DE ($w \lesssim -1.1$), if it occurs at all, is possible for moderately low redshifts $z < 0.4$ only and is favoured by the Gold+HST dataset, but not by the SNLS data.

This discrepancy may be a result of the different light-curve standardization techniques used by the two teams or due to systematic bias. Also, this could be due to the fact that the low redshift and high redshift SNe are obtained by different surveys. Future surveys such as SNAP [24], JEDI [25] and DUNE [26] should have a better handle on the systematic errors and such discrepancies should disappear.

We also attempt to obtain information on DE using datasets complementary to the supernova sample. To this end, we use information on the shift parameter R from the 3-year WMAP data and the quantity A for the baryon acoustic oscillation peak from SDSS. The results are consistent with ΛCDM but do not rule out weakly time dependent DE. These datasets appear to be rather sensitive to the value chosen for the present matter density $\Omega_{0\mathrm{m}}$. As a result, it is difficult to reach firm conclusion on the nature of DE from these data until strong model-independent constraints on $\Omega_{0\mathrm{m}}$ are obtained. Thus, even with the most recent data, the fundamental question if DE reduces to Λ or not, still remains open. On the other hand, possible deviation of DE properties from those of Λ is gradually becoming more and more restricted.

While this work was being finalised the paper [30] appeared containing results which are in broad agreement with ours in areas of overlap.

Acknowledgements

AS was partially supported by the Russian Foundation for Basic Research, grant 05-02-17450, and by the Research Program "Astronomy" of the Russian Academy of Sciences. He also thanks the Centre Emile Borel, Institut Henri Poincaré, Paris for the hospitality and the CNRS for partial support during the period when this project was finished.

[1] V. Sahni and A. A. Starobinsky, 2000, Int. J. Mod. Phys. **D 9**, 373 [astro-ph/9904398];
S M. Carroll, 2001, Living Rev.Rel. **4**, 1 [astro-ph/0004075];
P. J E. Peebles and B. Ratra, 2003, Rev.Mod.Phys. **75**, 559 [astro-ph/0207347];
T. Padmanabhan, 2003, Phys. Rep. **380**, 235 [hep-th/0212290];
V. Sahni, 2004, Lect. Notes Phys. **653**, 141 [astro-ph/0403324]; 2005, astro-ph/0502032;
S. Nojiri and S. D. Odintsov, 2006, hep-th/0601213;
R. P. Woodard, 2006, astro-ph/0601672;
E. J. Copeland, M. Sami and S. Tsujikawa, 2006, hep-th/0603057;
S. Bludman, 2006, astro-ph/0605198.
[2] V. Sahni and A. A. Starobinsky, 2006, astro-ph/0610026.
[3] A G. Riess, *et al.*, 2006, astro-ph/0611572.
[4] P. Astier *et al.*, 2005, Astron. Astroph. **447**, 31 [astro-ph/0510447].
[5] D. N. Spergel *et al.*, 2003, Astrophys.J.Suppl. **148**, 175 [astro-ph/0302209]; D N. Spergel et al, 2006, astro-ph/0603449.
[6] Y. Wang and P. Mukherjee, 2006, Astroph. J. **650**, 1 astro-ph/0604051.
[7] D. J. Eisenstein, *et al.*, 2005, Astroph. J. **633**, 560 [astro-ph/0501171].
[8] S. J. Perlmutter, et al., Nature **391**, 51 (1998).
[9] A. G. Riess, et al., Astron. J. **116**, 1009 (1998) [astro-ph/9805201].
[10] S. J. Perlmutter, et al., Astroph. J. **517**, 565 (1999) [astro-ph/9812133].
[11] J. L. Tonry, et al., 2003, Astroph. J. **594**, 1, [astro-ph/0305008].
[12] R. A. Knop, *et al.*, Astrophys.J. **598**, 102, (2003) [astro-ph/0309368].

[13] B. J. Barris, *et al.*, Astrophys.J. **602**, 571 (2004) [astro-ph/0310843].
[14] A. G. Riess, *et al.*, Astrophys.J. **607**, 665 (2005) [astro-ph/0402512].
[15] D. A. Howell, for the SNLS Collaboration, 2004, To appear in "1604-2004: Supernovae as Cosmological Lighthouses", Padua, June 16-19 2004, eds. Turatto et al., ASP conference Series.
[16] W. Hu and N. Sugiyama, 1996, Astroph. J. **471**, 30 [astro-ph/9510117].
[17] V. Sahni, T. D. Saini, A. A. Starobinsky and U. Alam, 2003, JETP Lett. **77** 201 [astro-ph/0201498];
U. Alam, V. Sahni, T. D. Saini and A. A. Starobinsky, 2003, Mon. Not. Roy. Ast. Soc. **344** 1057 [astro-ph/0303009].
[18] U. Alam, V. Sahni, T. D. Saini and A. A. Starobinsky, 2004, Mon. Not. Roy. Ast. Soc. **354** 275 [astro-ph/0311364].
[19] U. Alam, V. Sahni, T. D. Saini and A. A. Starobinsky, astro-ph/0406672.
[20] U. Alam, V. Sahni, A. A. Starobinsky, 2004, JCAP **0406** 008 [astro-ph/0403687].
[21] D. Huterer and A. Cooray, 2005, Phys. Rev. D **71**, 023506 [astro-ph/0404062].
[22] A. Shafieloo, U. Alam, V. Sahni and A. A. Starobinsky, 2006, Mon. Not. Roy. Ast. Soc. **366**, 1081 [astro-ph/0505329].
[23] S. Nesseris and L. Perivolaropoulos, 2005, Phys. Rev. D **72** 123519 [astro-ph/0511040].
[24] G. Aldering *et al.*, 2004, astro-ph/0405232.
[25] A. Crotts, et al., astro-ph/0507043.
[26] A. Refregier, et al., astro-ph/0610062.
[27] S. Nesseris and L. Perivolaropoulos, 2006, astro-ph/0610092.
[28] M. Chevallier and D. Polarski, 2001, Int. J. Mod. Phys. D **10**, 213 [gr-qc/0009008].
[29] E. V. Linder, 2003, Phys. Rev. Lett. **90**, 091301 [astro-ph/0208512].
[30] Y. Gong and A. Wang, astro-ph/0612196.

TABLE I: The reconstructed w-probe for the two different SNe datasets, Gold+HST and SNLS, using $\Omega_{0\mathrm{m}} = 0.28 \pm 0.03$

	$\bar{w}$		
Dataset	$\Delta z = 0 - 0.414$	$\Delta z = 0.414 - 1$	$\Delta z = 1 - 1.755$
Gold+HST	$-1.160^{+0.089}_{-0.070}$	$-0.226^{+0.319}_{-0.259}$	$0.268^{+0.073}_{-0.041}$
SNLS	$-1.037^{+0.069}_{-0.072}$	$-0.985^{+0.428}_{-0.296}$	

TABLE II: The reconstructed w-probe for the CMB+BAO dataset using three different marginalizations over $\Omega_{0\mathrm{m}}$

	$\bar{w}$		
$\Omega_{0\mathrm{m}}$	$\Delta z = 0 - 0.414$	$\Delta z = 0.414 - 1$	$\Delta z = 1 - 1.755$
0.25 ± 0.03	$-1.195^{+0.089}_{-0.070}$	$-0.948^{+0.319}_{-0.259}$	$-0.493^{+0.071}_{-0.041}$
0.28 ± 0.03	$-0.951^{+0.078}_{-0.072}$	$-0.779^{+0.428}_{-0.296}$	$-0.629^{+0.432}_{-0.296}$
0.31 ± 0.03	$-0.772^{+0.091}_{-0.079}$	$-0.819^{+0.394}_{-0.225}$	$-0.852^{+0.521}_{-0.535}$

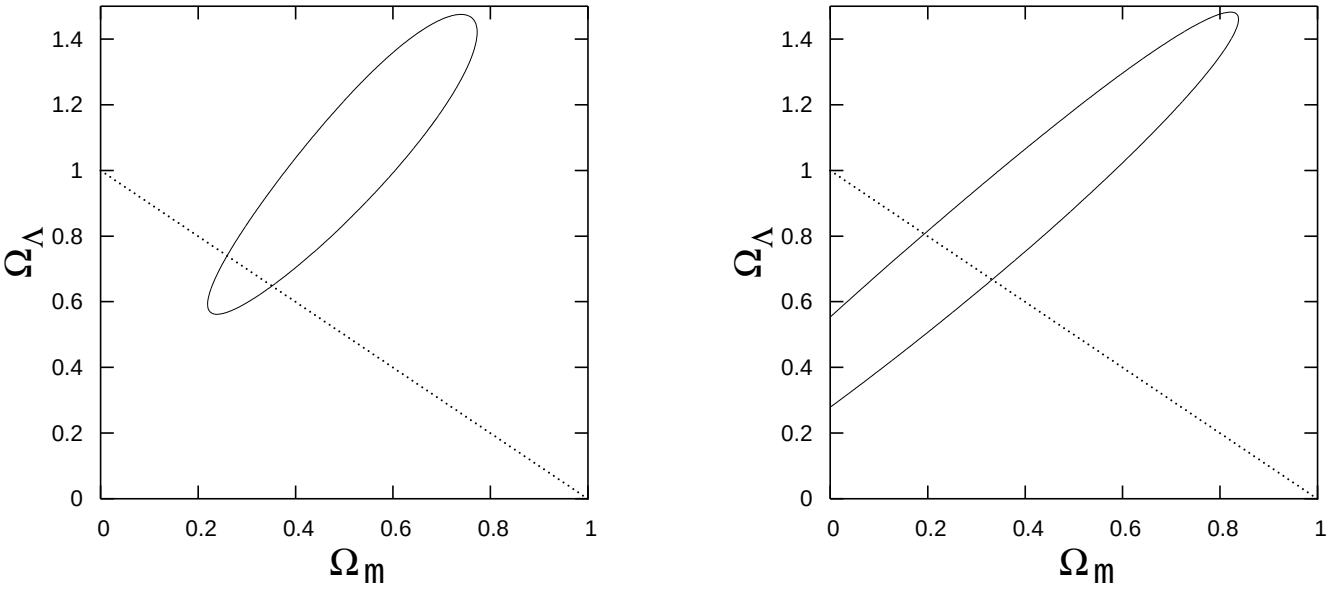

FIG. 1: 2σ confidence levels are shown for the Gold+HST dataset (left panel) and SNLS dataset (right panel) in the $\Omega_{0\mathrm{m}}, \Omega_\Lambda$ plane, with the dotted line showing the flat universe.

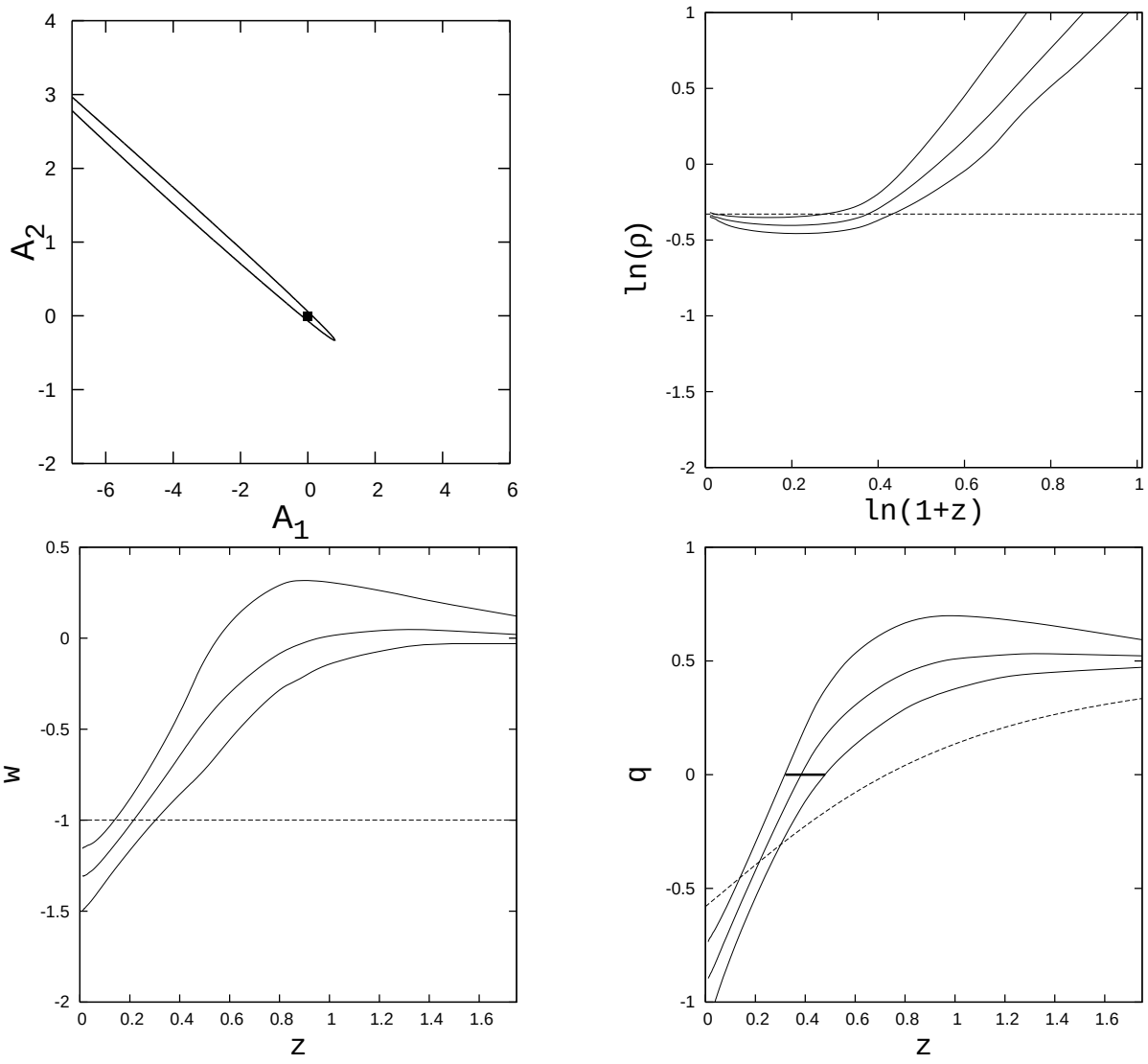

FIG. 2: 2σ confidence levels for the Gold dataset using $\Omega_{0\mathrm{m}} = 0.28 \pm 0.03$. The upper left hand panel shows the confidence levels in $A_1 - A_2$, with the black dot representing ΛCDM. The upper right hand panel shows the logarithmic 2σ variation of the DE density in terms of redshift. The dashed line represents ΛCDM. The lower left and right hand panels represent the variation of the equation of state and deceleration parameter respectively. The dashed lines in both panels represent ΛCDM. The thick solid line in the lower right hand panel shows the acceleration epoch, i.e. the redshift at which the universe started accelerating.

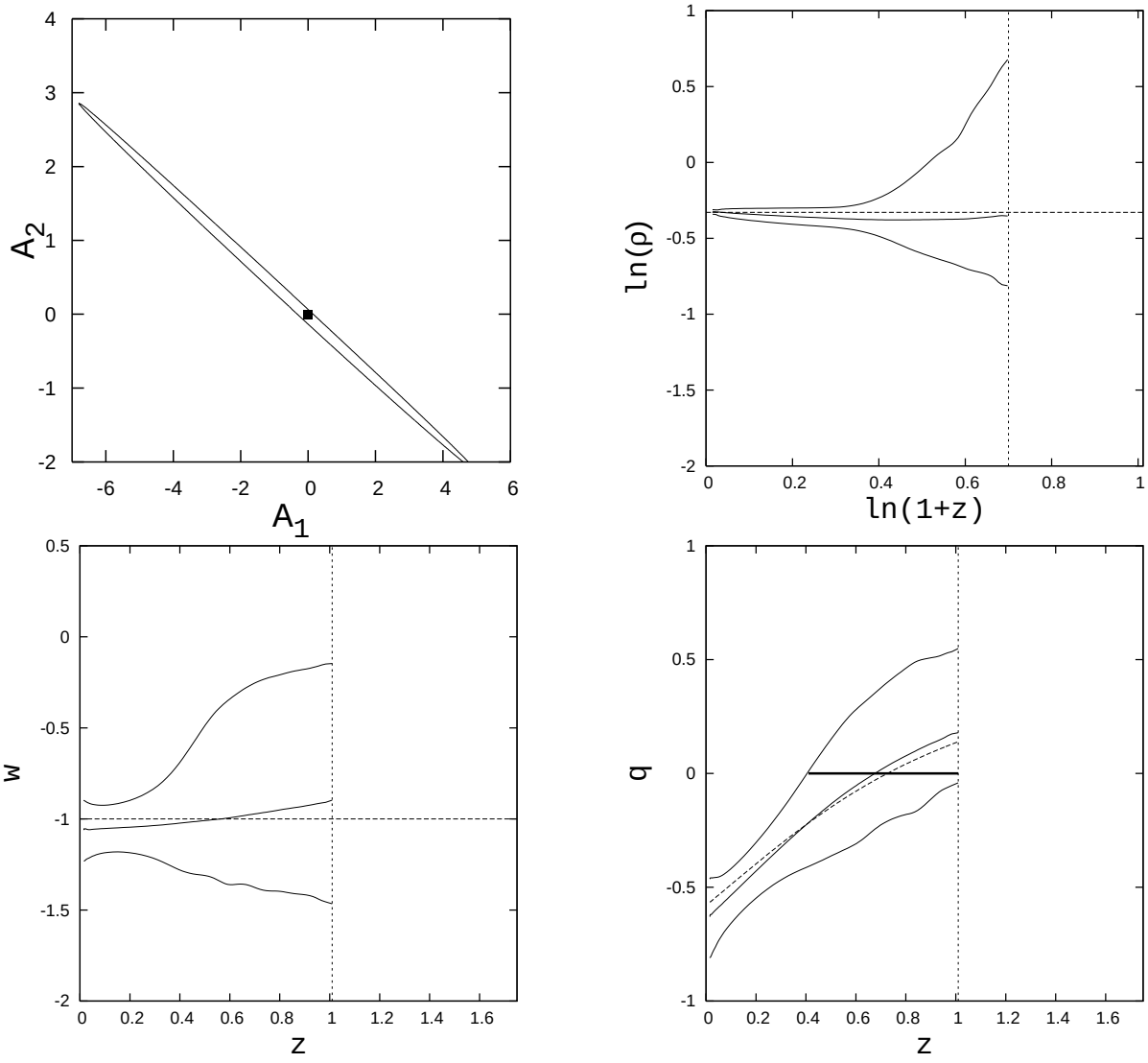

FIG. 3: 2σ confidence levels for the SNLS dataset using $\Omega_{0\mathrm{m}} = 0.28 \pm 0.03$. The upper left hand panel shows the confidence levels in $A_1 - A_2$, with the black dot representing ΛCDM. The upper right hand panel shows the logarithmic 2σ variation of the DE density in terms of redshift. The dashed line represents ΛCDM. The lower left and right hand panels represent the variation of the equation of state and deceleration parameter respectively. The dashed lines in both panels represent ΛCDM. The thick solid line in the lower right hand panel shows the acceleration epoch, i.e. the redshift at which the universe started accelerating. Results are shown upto $z = 1.01$

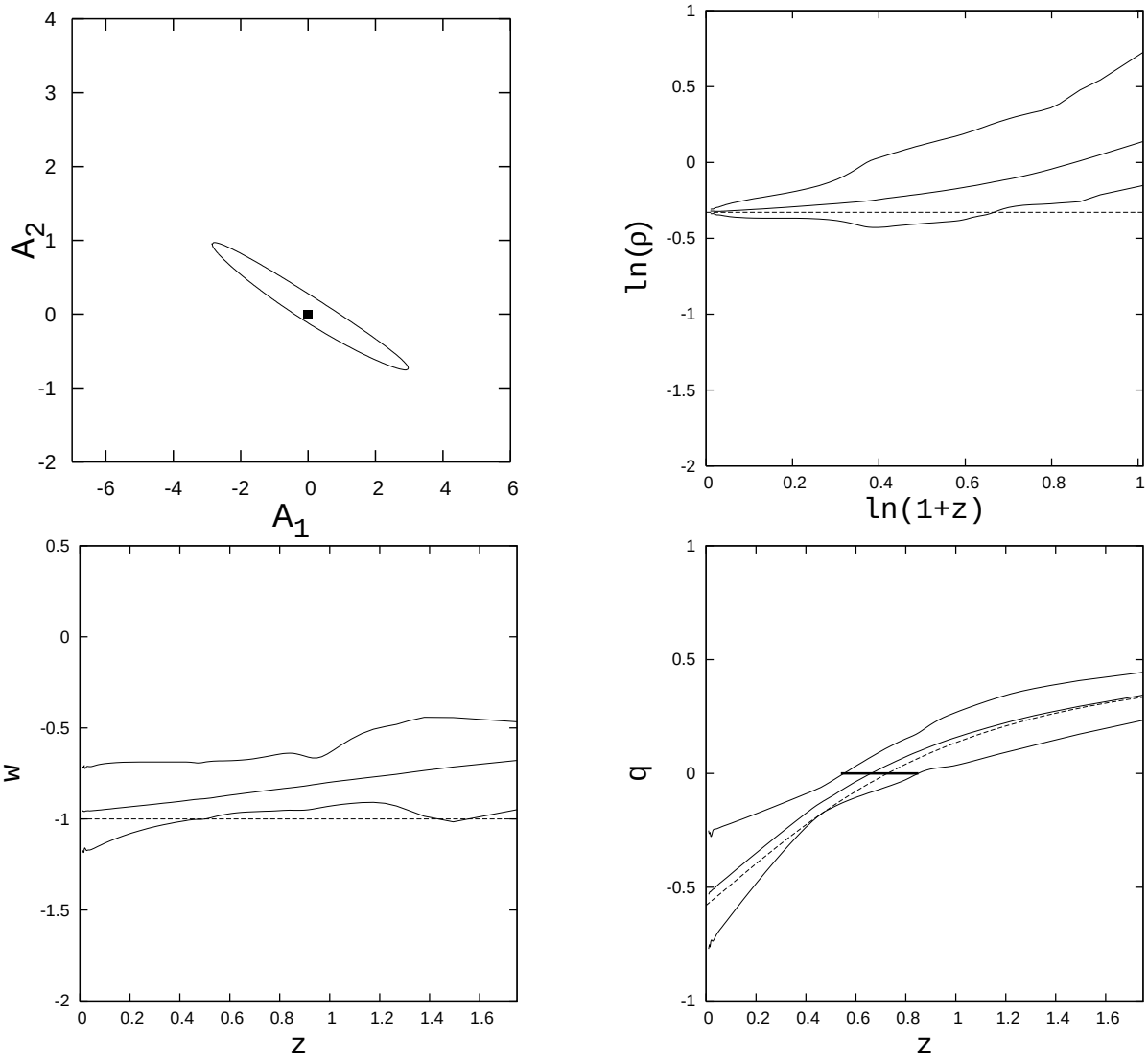

FIG. 4: 2σ confidence levels for the CMB+BAO dataset using $\Omega_{0\mathrm{m}} = 0.28 \pm 0.03$. The upper left hand panel shows the confidence levels in $A_1 - A_2$, with the black dot representing ΛCDM. The upper right hand panel shows the logarithmic 2σ variation of the DE density in terms of redshift. The dashed line represents ΛCDM. The lower left and right hand panels represent the variation of the equation of state and deceleration parameter respectively. The dashed lines in both panels represent ΛCDM. The thick solid line in the lower right hand panel shows the acceleration epoch, i.e. the redshift at which the universe started accelerating.

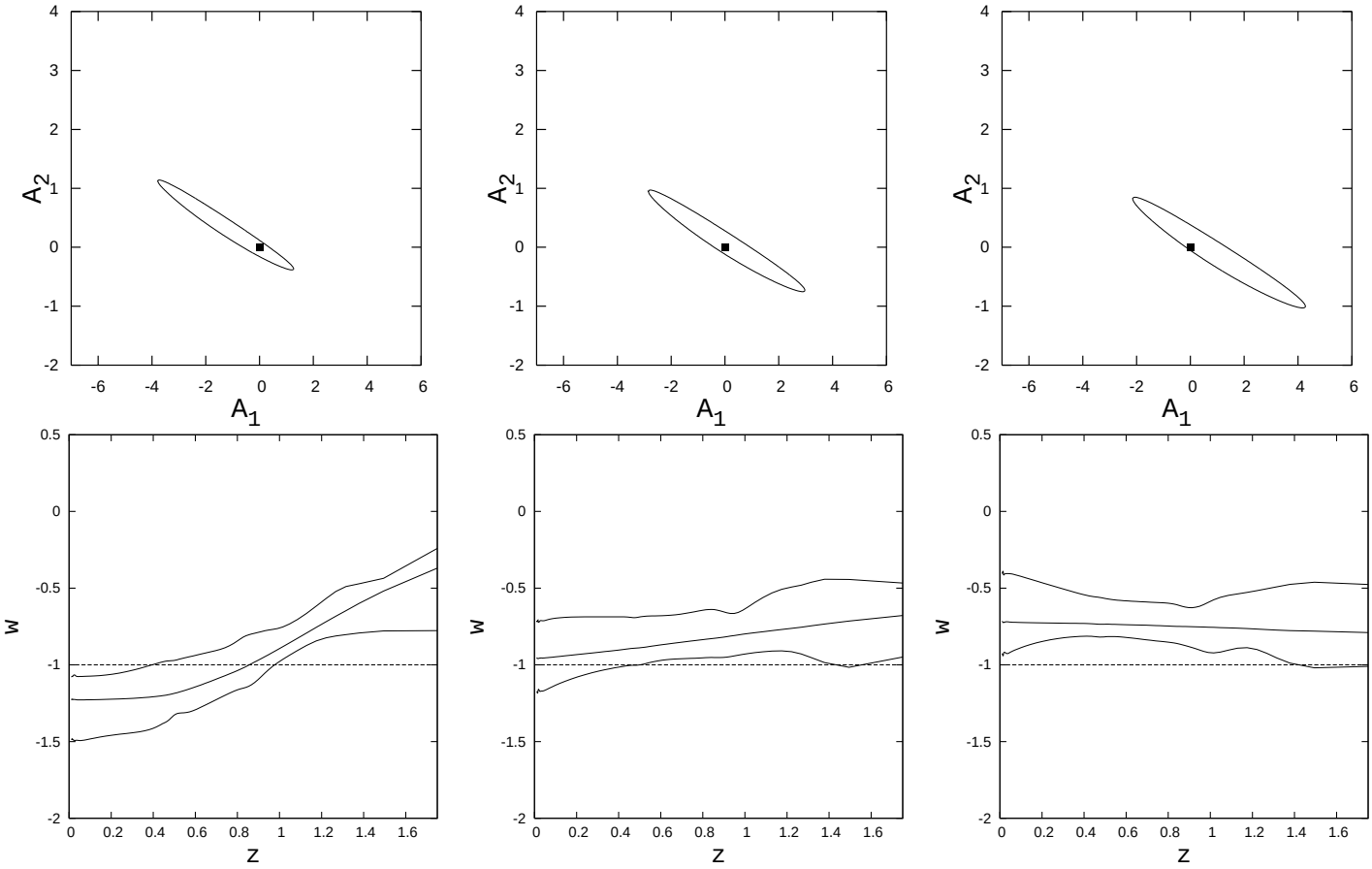

FIG. 5: 2σ confidence levels for CMB+BAO using different marginalizations over $\Omega_{0\mathrm{m}}$. The upper and lower left hand panels respectively show the confidence levels in $A_1 - A_2$ and the 2σ variation of w over redshift for $\Omega_{0\mathrm{m}} = 0.25 \pm 0.03$. The middle panels show the same for $\Omega_{0\mathrm{m}} = 0.28 \pm 0.03$ and the right-hand panels are results marginalized over $\Omega_{0\mathrm{m}} = 0.31 \pm 0.03$. The black dots in the upper panels and the dashed lines in the lower panels represent ΛCDM.

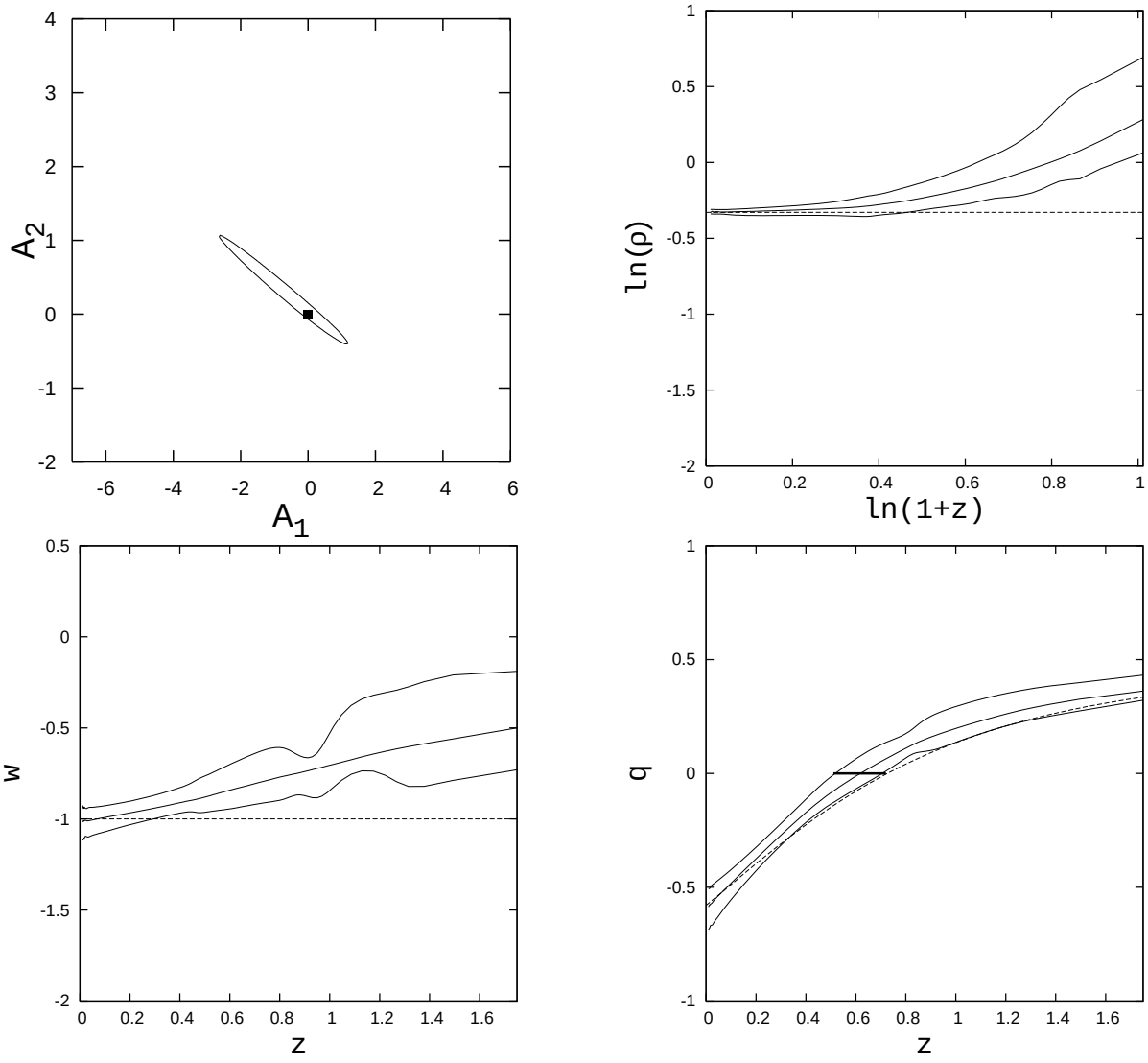

FIG. 6: 2σ confidence levels for the Gold+CMB+BAO dataset using $\Omega_{0\mathrm{m}} = 0.28 \pm 0.03$. The upper left hand panel shows the confidence levels in $A_1 - A_2$, with the black dot representing ΛCDM. The upper right hand panel shows the logarithmic 2σ variation of the DE density in terms of redshift. The dashed line represents ΛCDM. The lower left and right hand panels represent the variation of the equation of state and deceleration parameter respectively. The dashed lines in both panels represent ΛCDM. The thick solid line in the lower right hand panel shows the acceleration epoch, i.e. the redshift at which the universe started accelerating.

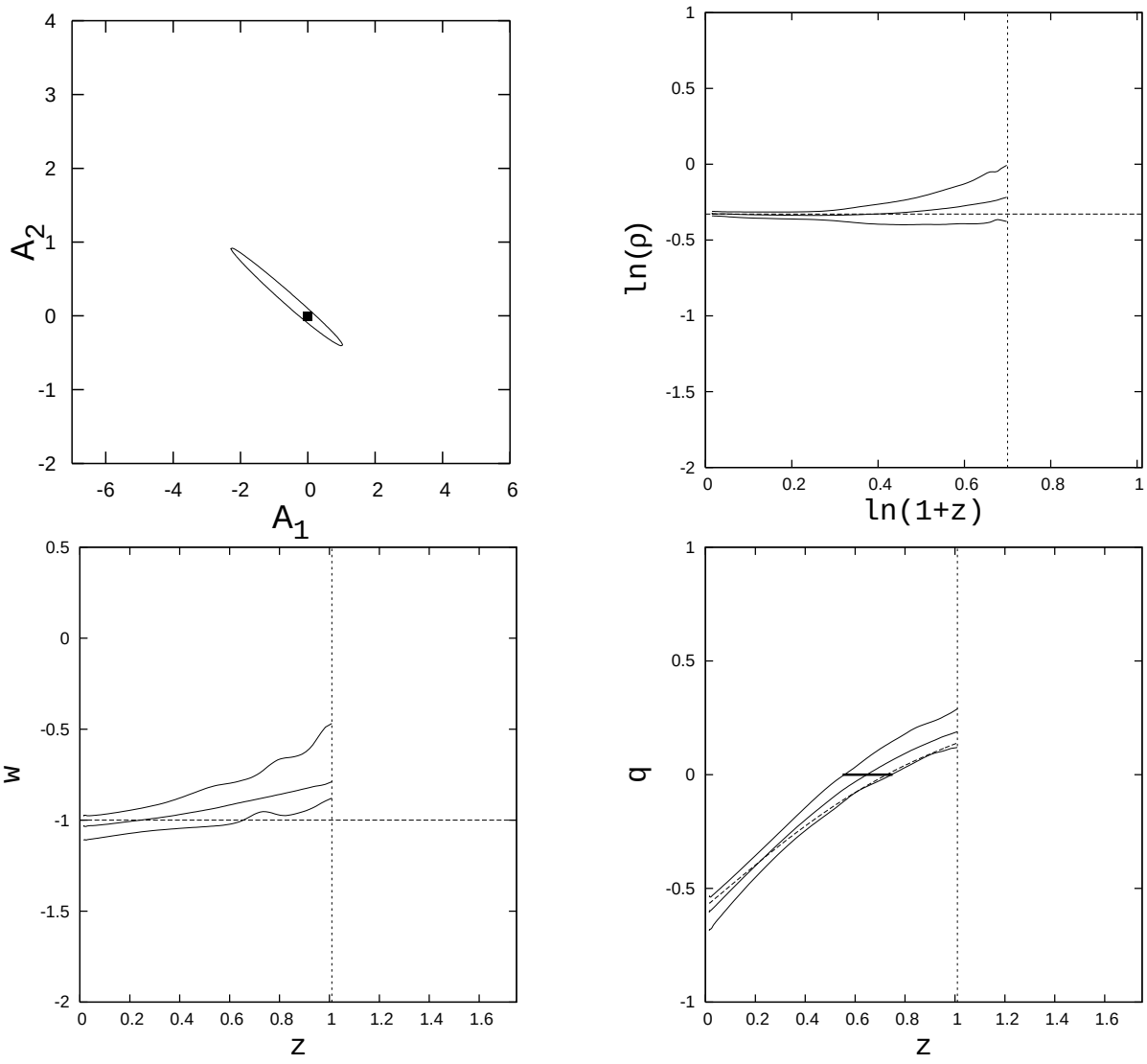

FIG. 7: 2σ confidence levels for the SNLS+CMB+BAO dataset using $\Omega_{0\mathrm{m}} = 0.28 \pm 0.03$. The upper left hand panel shows the confidence levels in $A_1 - A_2$, with the black dot representing ΛCDM. The upper right hand panel shows the logarithmic 2σ variation of the DE density in terms of redshift. The dashed line represents ΛCDM. The lower left and right hand panels represent the variation of the equation of state and deceleration parameter respectively. The dashed lines in both panels represent ΛCDM. The thick solid line in the lower right hand panel shows the acceleration epoch, i.e. the redshift at which the universe started accelerating. Results are shown upto redshift $z = 1.01$